Delay Tumor Growth Properties of LA-PEG-G Molecule and Its' Application as Drug Carrier

guangcheng wei (weiguangcheng2004@126.com)
Binzhou Medical University
Meixiu Xin
Binzhou Medical University
Hao Wang
Binzhou Medical University
Yehong Huo
Binzhou Medical University
Wei Hu
Binzhou Medical University
Jigang Jiang
Binzhou Medical University
Lei Wang
Binzhou Medical University
Liying Ma
Binzhou Medical University
Miaomiao Yan
Binzhou Medical University
Chunhua Wang
Binzhou Medical University

Research

Keywords: Linoleic acid, PEG, Guanosine, nanomedicine, Anticancer

Posted Date: January 22nd, 2020

DOI: https://doi.org/10.21203/rs.2.21548/v1

Delay Tumor Growth Properties of LA-PEG-G Molecule and Its' Application as Drug Carrier

Guangcheng Wei[*,†], Meixiu Xin[†], Hao Wang, Yehong Huo, Wei Hu, Jigang Jiang, Lei Wang, Liying Ma, Miaomiao Yan, Chunhua Wang[*]

Department of Pharmacy Science, Binzhou Medical University, Yantai, 264003, China

† These authors are equal to the contribution of this work.

*Correspondence authors E-mail: weiguangcheng2004@126.com;

chhuawang2018@126.com

Abstract

LA–PEG–G molecule was prepared through the covalent conjugation of linoleic acid, polyethylene glycol and guanosine. LA–PEG–G molecule can self-assemble into spherical aggregate in aqueous solution. The size of the LA–PEG–G aggregate was approximately 132.1 ± 13.718 nm, and the Zeta potential was −36.3 ± 0.9644 mv. The loading rate of LA–PEG–G aggregates to Dox was 84.62 ± 1.810%. In vitro release experiments showed that Dox release from the LA–PEG–G–Dox nanomedicine was slow-release. Cell experiments showed that LA–PEG–G aggregates have low cytotoxicity, and the relative cancer cells survival rate decreased with the increasing of time and LA–PEG–G–Dox nanomedicine concentration. In vivo experiments showed that LA–PEG–G–Dox nanomedicine can inhibit tumor growth, and the LA–PEG–G aggregate could also delay the tumor growth which is very important to play the synergistic antitumor effect with the anticancer drug. Serum biochemistry showed that LA–PEG–G–Dox nanomedicine which reduced the Dox toxicity had very good antitumor effect. The tumor tissue sections indicated that LA–PEG–G–Dox nanomedicine can effectively induce tumor cell apoptosis, and finally cause tissue necrosis to achieve tumor treatment.

Key words: Linoleic acid; PEG; Guanosine ; nanomedicine ; Anticancer

1. Introduction

The global incidence of cancer is increasing yearly, and cancer has become an

important cause of death in humans. Therefore, cancer treatment is important[1]. Traditional cancer treatment includes surgery, radiotherapy, chemotherapy, and subsequent biological treatment. Different methods have different applicability to different cancers or stages of cancer. Chemotherapy can quickly inhibit the rapid growth of tumor cells, but damaged tumor cells still differentiate faster than normal cells. Moreover, the side effects of chemotherapy are seriously large and toxic due to the nonspecificity treatment of anticancer drugs. Therefore, new green therapies need to be discovered to reduce the side effects of traditional cancer treatment is an urgent problem to be solved[2]. Various drug carriers provide a solution to the above problems[3-6]. Drug carriers can change the pharmacokinetic properties of the chemotherapy drug. For example, it can improve the water solubility of the drug, prolong the systemic circulation time, and avoid nonspecific uptake and preferential accumulation of tumor sites by enhancing osmotic and retention effects[7].

The materials used in drug carriers affect the properties of drug carriers. Linoleic acid (LA) is a polyunsaturated fatty acid containing two unsaturated fatty chains with various good biological properties[8-9]. In addition, polyunsaturated fatty acids have been found to have antitumor properties and sensitivity to cancer cells and exhibit potential tumor therapeutic effects. Polyethylene glycol (PEG) has excellent water solubility and biocompatibility and can significantly prolong the circulation time[10] in the body systemic circulation. PEG can form a water layer on the surface of the polymer, thereby increasing the stability of the polymer and reducing the adsorption of proteins in the body and reducing the recognition of the mononuclear macrophage system as much as possible. Long-circulating macromolecules and various long-circulating nanomedicines spontaneously accumulate in pathological areas (such as tissue sites) that have high permeation and retention effects (EPR effect)[7,11]. Therefore, the PEG-modified aggregates easily aggregate at the tumor site, endowing the passive targeting effect of the aggregate. Guanosine (G) is an important extracellular signal molecule secreted by astrocytes. When the central nervous system is damaged, the extracellular G concentration in this region is instantly increased, and a variety of important cellular pathways are activated to counteract brain damage[12-16].

In addition, G can regulate the metabolism of glutamate and avoid the excitatory poisoning caused by excessive excitation of glutamate receptors. Simultaneously, the anti-oxidation and anti-inflammatory effects of G can regulate a variety of cellular pathways to protect the central nervous system[17,18]. Further studies found that the nutritional and central defense function of G can also alleviate chronic diseases such as depression and Parkinson's disease[19].

In the present study, the LA–PEG–G was prepared through the covalent conjugation of LA, PEG, and G molecules **(Scheme 1)**. The LA–PEG–G molecules can self-assemble into spherical aggregates in aqueous solution, and the potential targeting of LA combined with the EPR effect of PEG can increase the targeting and prolong the cycle time of LA–PEG–G aggregate. The spherical LA–PEG–G aggregates can load the lipophilic anticancer drugs. Dox was used as a drug model to obtain LA–PEG–G–Dox nanomedicine. Dox release from the LA–PEG–G–Dox nanomedicine was pH-responsive and slow-release. Moreover, in vivo and in vitro experiments showed that the LA–PEG–G–Dox nanomedicine can induce apoptosis in the cell of tumor tissue to inhibit tumor growth and metastasis. The LA–PEG–G drug carrier adds new impetus to the development of drug delivery systems and is expected to contribute to clinical applications.

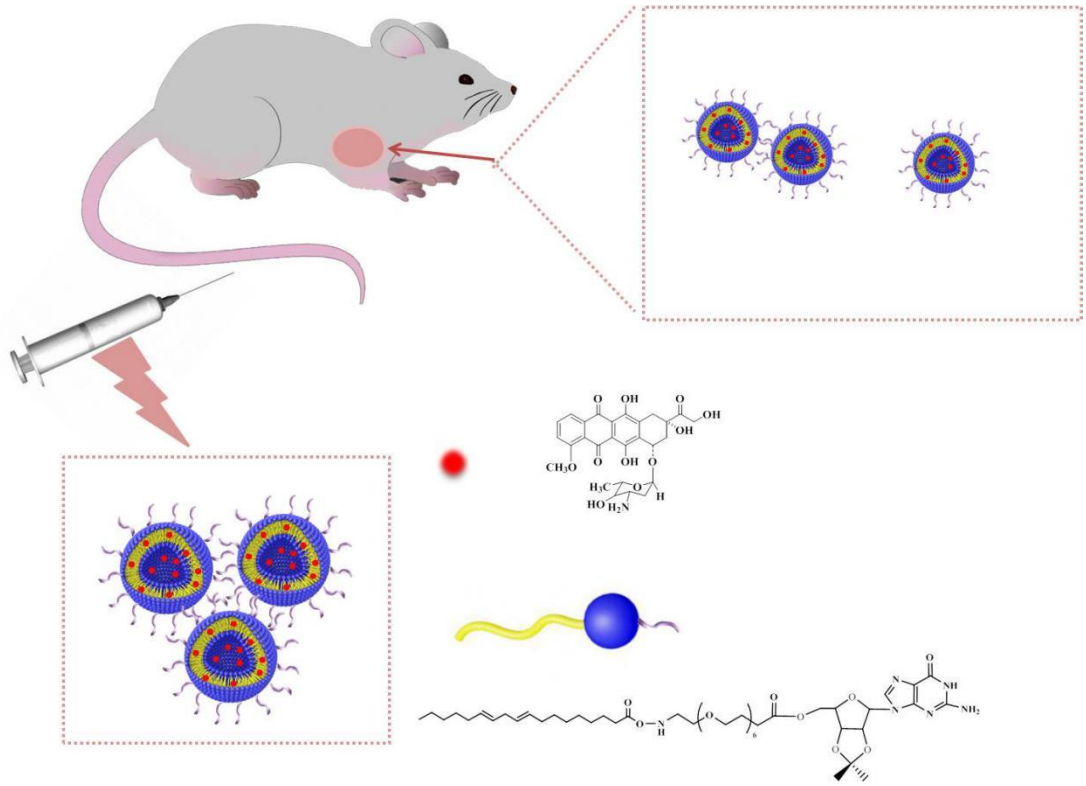

Scheme 1 LA–PEG–G molecules self-assemble into spherical aggregates that are used as drug delivery systems for tumor treatment.

2. Experimental and Methods

2.1 Synthesis of LA–PEG Molecules

The LA (0.08797 mL, 0.2830 mmol. J&K Scientific, China) was dissolved in 15 mL anhydrous THF while stirring. Then, DCC (0.03396 mmol. N, N′-dicyclohexylcarbodiimide) and NHS (0.03396 mmol. N-hydroxysuccinimide) were added into the above THF solution and dissolved while stirring for 24 h at room temperature. After the prescribed time, 15 mL of DMF which contained PEG (1-amino-3,6,9,12,15,18-hexaoxahenicosan-21-oic acid) at 100 mg (0.2830 mmol) was added into the above THF mixture and then reacted for 48 h while stirring at room temperature. Then, the mixture solution was filtered to remove any solid matter, and the solution was retained and subjected to freeze-drying treatment to obtain a white LA–PEG crude powder(Scheme 2). The LA–PEG crude powder was purified by silica gel column chromatography with the mobile phase of dichloromethane and methanol, and the elution of 97 to 3 (Dichloromethane to methanol) was collected. The elution was then freeze-dried to give a pale yellow LA–PEG powder pure sample.

2.2 Synthesis of LA–PEG–G Molecules

G (2',3'-isopropylidene Guanosine; 100.6246 mg, 0.283 mmol) was dissolved in 15 mL anhydrous DMF. Then, DIPEA (283 μL), DMAP (0.03457 g, 0.283 mmol) and EDC (0.05425 g, 0.2830 mmol) was added while stirring. The LA–PEG sample was firstly dissolved in 15 mL of anhydrous DMF. Then, the LA–PEG DMF solution was mixed with the above G mixture solution and then stirred for 48 h at room temperature[20] (**Scheme 2**). The crude product of LA–PEG–G was obtained and purified by alkaline alumina column chromatography with the mobile phase of methanol to ethyl acetate. The elution solution of 1:1 (Methanol: ethyl acetate) was collected and then lyophilized to obtain the pure sample LA–PEG–G molecules.

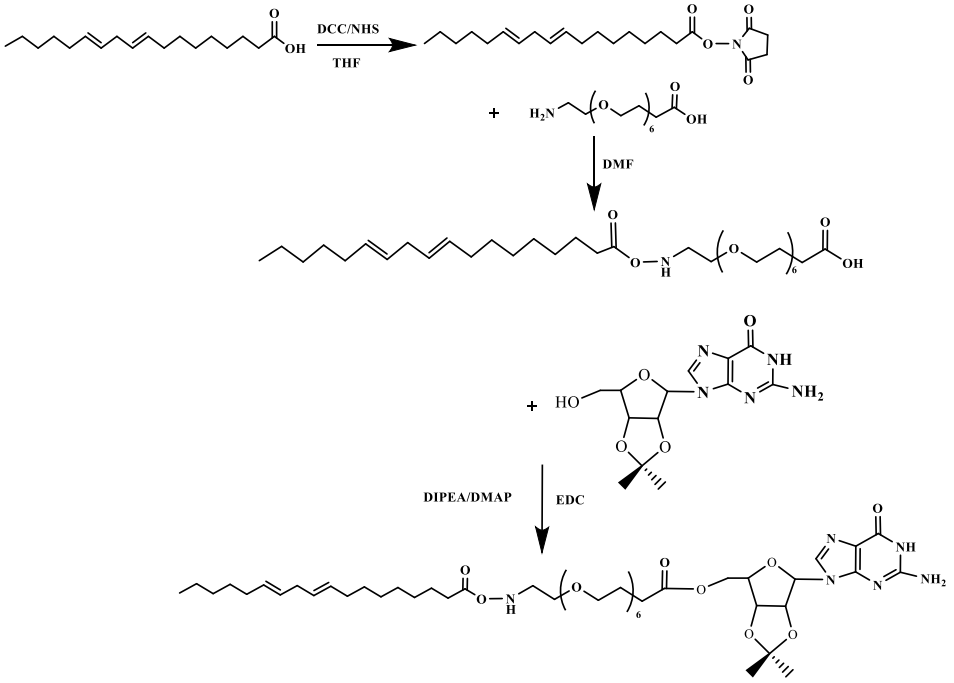

Scheme 2 The synthetic process of LA–PEG–G molecules

2.3 Determination of Critical Aggregation Concentration of LA–PEG–G Aggregates

LA–PEG–G can self-assemble to form aggregates in aqueous solution. The critical aggregation concentration (CAC) measurement of aggregates was carried out by the fluorescence probe method to study the aggregation process of LA–PEG–G in water. The pyrene fluorescent probe is a hydrophobic molecule. The fluorescence spectrum of the pyrene molecule has a significant change in different solvents, and the CAC value[21] is judged based on the significant change of the fluorescence spectrum.

Pyrene was dissolved in acetone to prepare a mother liquor of 50 μL 6×10^{-6} mol·L^{-1}, which was added to nine volumetric flasks (10 mL). Then, a series concentration of LA–PEG–G aggregate solution was added to the volumetric flask. Finally, the solution was filled to the mark with distilled water. The concentration of the LA–PEG–G aggregate solution was 1×10^{-6}–1×10^{-1} mg·mL^{-1}, and then sonicated for 30 min, and then incubated for 30 min at 50 °C. Finally, the fluorescence spectrum (LS-55, PerkinElmer, UK) was measured, and the excitation and emission wavelength was 295 and 339 nm respectively. Moreover, the excitation and emission slit was 5 and 2.5 nm, respectively. The CAC value[21] was determined by the change of the ratio of I_{371} (I refers to fluorescence intensity) to I_{391} in the fluorescence spectrum[21].

2.4 Morphology Observation of LA–PEG–G Aggregates and the Determination of Particle Size and Zeta Potential

LA–PEG–G molecules can self-assemble to form aggregates in water. The particle size and morphology were determined to verify the distribution in LA–PEG–G aggregates. The morphology of LA–PEG–G aggregates was characterized by TEM (Transmission electron microscopy. JEM-1400, JEOL, Tokyo, Japan). The LA–PEG–G aggregate solution was dropped onto the copper mesh with carbon support film and kept on the copper mesh for 2 min. The liquid on the copper mesh was sucked off from the filter paper on one side. Then, the aggregates on the copper mesh were subjected to negative staining with 1 % phosphotungstic acid. The copper mesh was placed under the infrared lamp for drying treatment after negative dyeing, and TEM characterization[22]was performed. The particle size and Zeta potential of the aggregates were measured by a Marvin particle sizer (Zeta sizer Nano ZS, UK).

2.5 Preparation of LA–PEG–G–Dox Nanomedicine and Determination of Encapsulation Efficiency

1 mg Doxorubicin (Dox) was added into 10 mL methanol. Then, 480 μL triethylamine (The molar ratio of Dox to triethylamine is 1 to 2) was added while stirring for 6 h in the dark place. Then, the methanol solution which contained 1 mg LA–PEG–G sample was added to the above mentioned mixture solution with stirring and then incubated for 30 min at 50 °C. After the prescribed time, the methanol was removed

by using a rotary evaporator. The mixture was then mixed with 25 mL of distilled water, sonicated for 1 h, and then centrifugated (12 000 rpm, 5 min). The absorbance intensity of the supernatant was determined with the ultraviolet–visible (UV-vis) spectrophotometer (The measuring wavelength is 485 nm), and the encapsulation efficiency was calculated according to the Dox standard absorption curve. The encapsulation rate calculation formula is as follows:

$$EE\% = \left(1 - \frac{C_{sup}}{C_{tol}}\right) \times 100\%$$

where C_{sup} is the concentration of Dox in the supernatant solution and C_{tol} is the total concentration of Dox.

2.6 The Release Behavior of Dox from the LA–PEG–G–Dox Nanomedicine

Dox is a broad-spectrum anticancer drug which can inhibit the synthesis of RNA and DNA through intercalating nucleic acid. Therefore, whether Dox can be released from LA–PEG–G–Dox nanomedicine is a prerequisite for Dox to function. Therefore, studying the in vitro release of Dox from the LA–PEG–G–Dox nanomedicine is necessary. The infinite proliferation of tumor cells leads to hypoxia in tumor tissues, and glycolysis produces a large amount of lactic acid in an anaerobic state. Therefore, the pH in tumor tissues is lower than that in normal tissues. Hypoxia and acidic microenvironment become prominent features of tumor tissue[23]. According to the micro-acid environment of the tumor tissue, the pH-targeting carrier can be designed to make the Dox, which enters and accumulates primarily in the tumor tissue to better exert the antitumor effect. The release behavior of Dox from the LA–PEG–G–Dox nanomedicine at pH 5.0 and 7.4 was investigated to study the effect of tumor microenvironment on the release behavior. The amount of Dox released was measured at 37 °C. Buffer solution (4 mL) was taken out from the buffer solution outside the dialysis bag for UV–visible spectrophotometer detection (detection wavelength is 485 nm) at different times (1, 2, 4, 8, 12, 24, 36, 48, 72, 84, 96, 108, and 120 h), whereas 4 mL fresh buffer solution was added into the buffer solution outside the dialysis bag. The released Dox concentration was calculated according to the standard curve of Dox, and the cumulative release amount was finally calculated according to the

following formula:

$$\text{Accumulated Release Percentage} = \frac{n_i C_i V + \sum n_{i-1} C_{i-1} V_{extract}}{W} \times 100\%$$

In this equation, n_i is the fold of dilution, C_i is the DOX concentration in each sample, V means the medium volume (20 mL), $V_{extract}$ is sample volume (1.0 mL), and W represents the total amount of Dox.

2.7 Cell culture

The human liver cancer (HepG2 cells) and breast cancer cell lines (MCF-7 cells) were selected as experimental cell models to analyze the cytotoxicity of LA–PEG–G aggregates and the anticancer activity of LA–PEG–G–Dox nanomedicines. Both cells were obtained from the experiment center of Binzhou Medical University. HepG2 and MCF-7 cells were incubated in DMEM high-glucose culture medium, which contained 10 % fetal bovine serum and 1 % penicillin and streptomycin (penicillin, 100 $U \cdot mL^{-1}$; streptomycin, 0.1 $mg \cdot mL^{-1}$) in 5 % CO_2 atmosphere at 37 °C.

2.8 Cell Cytotoxicity of LA–PEG–G Aggregates and the Anticancer Activity of LA–PEG–G–Dox Nanomedicine

HepG2 and MCF-7 cells are commonly used as model cells to verify the anticancer activity of LA–PEG–G–Dox nanomedicine. In this experiment, MTT (3-[4,5-dimethyl-2-thiazolyl]-2,5-diphenyl-2-H-tetrazolium bromide) method was used to assess the effect of LA–PEG–G aggregates and LA–PEG–G–Dox nanomedicine on cell viability of both cells. HepG2 and MCF-7 cells were seeded into 96-well plates (about 5×10^4 per well), and 200 μL culture medium was added to each well. The culture medium contained 10 % fetal bovine serum and 1 % penicillin and streptomycin. The cells were cultured overnight in 5 % CO_2 incubator at 37 °C until the cells adhered. Then, the old culture medium was removed. A series of concentration gradients of LA–PEG–G aggregates and LA–PEG–G–Dox was added. Untreated cells served as control group. The cells were then placed in an incubator to incubate for 24 h. After 24 h, MTT was added to 96-well plate at 10 μL per well and incubated for another 4 h. After the prescribed time, all the old culture solutions in each well were removed. Then, 150 uL of DMSO was added to each well, and the

96-well plate was shaken for 10 min in the dark. Finally, the absorbance intensity was determined with the microplate reader at detection wavelength of 570 nm. The cell survival rate is calculated as follows:

$$\text{Cell survival rate (\%)} = \frac{\text{OD}_{\text{treated}}}{\text{OD}_{\text{control}}} \times 100\%$$

Where $OD_{treated}$ and $OD_{control}$ are the absorbance intensities for the experimental group and control group, respectively. Each sample was determined three times.

2.9 Cell Uptake

2.9.1 Laser-Scanning Confocal Microscopy (LSCM)

HepG2 cells were chosen as experimental model cells to study the uptake of LA–PEG–G–Dox nanomedicine by cancer cells. HepG2 cells were seeded in 6-well plates (The number of cells per well was approximately 1×10^{-5}) and then mixed with 2 mL culture medium containing 10% fetal bovine serum and 1 % penicillin and streptomycin per well. The cells were cultured overnight in 5 % CO_2 incubator at 37 °C until the cells adhered, and the old culture solution was removed. LA–PEG–G–Dox nanomedicine was added, and the final concentrations were 10μg·mL^{-1} and 20 μg·mL^{-1}. Cells were cultured for 4 h, 8 h, and 24 h respectively. After the prescribed time, the old culture solution was removed and washed there time with PBS (1×) to prevent the excess LA–PEG–G–Dox nanomedicine in the plate from affecting the experimental results. Finally, 2 mL of the fresh culture medium was added. The Petri dishes were transferred to laser-scanning confocal microscopy (LSCM, EPICS XL, Beckman, USA) for measurement. The excitation and emission wavelengths were 488 nm and 590 nm nm respectively.

2.9.2 Flow Cytometry (FCM)

LSCM can qualitatively study the uptake of LA–PEG–G–Dox nanomedicine in cancer cells. Flow cytometry (FCM) was used to further quantitatively study the uptake of LA–PEG–G–Dox nanomedicine in cancer cells. HepG2 cells were seeded in 6-well plates (the number of cells per well was approximately 1×10^{5}), and then, 2 mL culture medium containing 10 % fetal bovine serum and 1 % penicillin and streptomycin was added to each well. The cells were cultured overnight in a 5 % CO_2

incubator at 37 °C until the cells adhered, and the old culture medium was removed. Then, the LA–PEG–G–Dox nanomedicine was added, and the final concentrations were 10μg·mL^{-1} and 20 μg·mL^{-1}. The cells were then cultured for 4 h, 8 h, and 24 h. After the prescribed time, the old culture medium was removed and then washed three time with PBS (1×). 1 mL Trypsin was added to each well to digest the cells. After 2 min, the collected old culture solution was added to prevent digestion and gently triturated to make the cell suspension. The cells were transferred to a flow tube for FC determination (TCS SPE, Leica, Germany). The excitation and emission wavelengths were 488 and 590 nm respectively.

2.10 Animal Experiment and Blood Chemistry

Ethics approval and consent to participate: The experimental protocol was established, according to the ethical guidelines of the Helsinki Declaration and was approved by the Human Ethics Committee of Binzhou Medical University. Written informed consent was obtained from individual or guardian participants.

2.10.1 Antitumor Activity of LA–PEG–G–Dox Nanomedicine in Mice

Tumor-bearing mice were used as experimental models to further study the antitumor effect of LA–PEG–G–Dox nanomedicine in vivo. All the mice (30–35 g) used in the trial were female and housed under the "Guidelines for the Care and Use of Test Animals." When the mice growed for 4–6 weeks, the left forelimb was depilated to expose, and then H22 cells (1×10^6) were injected into the left subcutaneous forelimb. The following experiment was carried out when the tumor volume has grown to 100–200 mm^3. The mice were randomly divided into four groups, namely, the PBS group, Dox group, LA–PEG–G aggregate group, and LA–PEG–G–Dox nanomedicine group. The PBS (0.2 mL), Dox (15 mg·kg^{-1}), LA–PEG–G aggregate (15 mg·kg^{-1}), and LA-PEG-G-Dox nanomedicine (15 mg·kg^{-1}) were injected separately into the mice body through the tail vein injection every other day. The mice body weight were weighed before injection, and the mice volume was also measured with a vernier caliper. The mice blood were obtained by using the neck-breaking method at the end of the experiment. The tumor, heart, liver, spleen, lung, and kidney were dissected. All dissected tissues were immediately placed in paraformaldehyde (4 %) to fix for 48 h.

After the prescribed time, the tissues were dehydrated, embedded in paraffin, sliced, and then stained with Hematoxylin-Eosin (HE).

2.10.2 Blood Serum Chemistry

After 19 days injection to the mice, the whole-body blood was collected through the neck-breaking method. The blood was allowed to coagulate for 20–30 min at room temperature and then centrifuged at 3500 r/min for 5 min. The supernatant was collected to execute the analysis of the liver function, renal function, and myocardial enzyme.

2.11 Statistical Analysis

Statistical analysis was performed using the Student *t*-test. The significance level was set as $p < 0.05$.

3. Results and Discussion

3.1 Synthesis, Characterization, and Aggregation Behavior of LA–PEG–G Molecules

The pure LA–PEG–G sample was obtained through the purification of column chromatography. Thin-layer chromatography was used to preliminarily analyze the LA–PEG–G sample. The Rf value of LA–PEG–G sample was obviously different from those of LA, DCC, NHS, and PEG molecules as shown in **Figure S1**, which preliminarily proved that the sample was the LA–PEG–G sample. The LA–PEG–G molecules were characterized through the FT-IR (Fourier transform infrared spectroscopy), nuclear magnetic resonance (NMR) and mass spectrometry (MS) methods. As seen from the FT-IR spectrum**(Figure S2)**, the 1568 cm^{-1} peak was the characterization of stretching vibration of –C=C– group of LA molecules, and the 648 cm^{-1} peak was the *cis*-hydrocarbon stretching vibration peak of –C=C– group of LA molecules, and the peak at 3435 cm^{-1} was the stretching vibration of –NH– group of G, and the peak at 1614 cm^{-1} was the stretching vibration peak of the carbonyl bond of PEG molecules. The above FT-IR results showed that the LA–PEG–G molecules were successfully synthesized. As shown in the NMR spectrum **(Figure S3)**, δ 8.56 was the H shift of –NH– group in G, and δ 7.81 was the H shift of –NH– group, which was formed by the LA and PEG molecules, respectively. Moreover, δ5.58–4.40 was the H

shift on the side chain of five-membered ring of G, and δ 4.90 was the H shift of $–NH_2$ group in G. All NMR data showed that the LA–PEG–G molecules were successfully synthesized. The MS spectrum showed that the 964.36 (m/z) peak was the negative ion peak of $[M+HCOOH]^-$, thereby indicating that the LA–PEG–G molecules had been successfully synthesized. In summary, the NMR spectrum and MS proved that LA–PEG–G molecule had been successfully synthesized. The successful synthesis of LA–PEG–G molecules was the prerequisite for further experiment.

LA is a typical fat-soluble molecule, and PEG is a hydrophilic polymer, which make the LA–PEG–G molecule exhibit both lipophilic and hydrophilic properties. The property of the LA–PEG–G molecule allows it to self-assemble into spherical aggregates in water. The CAC value of the LA–PEG–G molecules was $2.512\times10^{-3}mg\cdot mL^{-1}$ **(Figure S5)**. The morphology of LA–PEG–G aggregates was observed with the TEM and FF-TEM (Freeze-fracture TEM), as shown in Figure 1a and 1b. The LA–PEG–G aggregates exhibited a spherical structure with uniform shape and distribution without aggregation. The size of LA–PEG–G aggregates was about 40 nm, as shown in the **Figure 1b**. However, the results of Malvern particle size analyzer showed that the size of the LA–PEG–G aggregates in aqueous solution was 132.1 ± 13.72 nm as shown in Figure 1c. The hydration radius of LA–PEG–G aggregates is the size difference to the results of FF-TEM. The size of aggregates allows easy accumulation in the tumor tissue through the EPR effect. The Zeta potential of the LA–PEG–G aggregates was −35.80 mV in the aqueous solution, which indicated that the surface of the LA–PEG–G aggregates was negatively charged in aqueous solution. A high Zeta potential allows the LA–PEG–G aggregates to maintain good dispersion in aqueous solution[24,25]. The PEG in the LA–PEG–G molecules can help the LA–PEG–G aggregates escape from the trap of Kupffer cells and macrophages in the spleen through scavenger receptors without activating MPS, which help the blood circulation of the LA–PEG–G aggregates in the body[25].

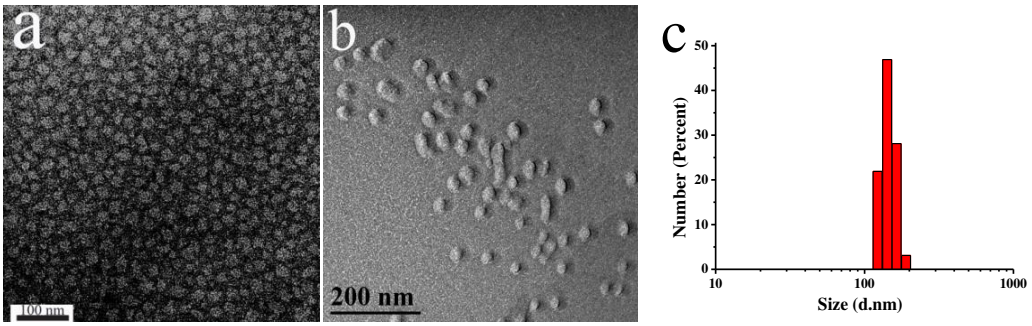

Figure 1. Characterization of the morphology and particle size distribution of LA–PEG–G aggregates. (a) TEM image of LA–PEG–G aggregates; (b) FF-TEM image of LA–PEG–G aggregates; (c) Particle size distribution of LA–PEG–G aggregates.

3.2 Dox-Loading Ratio of LA–PEG–G Spherical Aggregates and Dox Release Behavior from the LA–PEG–G–Dox Nanomedicine

Dox is a broad-spectrum antitumor antibiotic which can insert into DNA helical double chain and thereby affects DNA transcription and protein synthesis, which cause the strong toxicity (Such as cardiotoxicity, nausea, and loss of appetite)[26]. The encapsulation of LA–PEG–G aggregates to Dox decreases its toxicity, and improves its water solubility, and facilitates its intravenous injection. The encapsulation results showed that the loading ratio of LA–PEG–G aggregates to Dox was 81.77 % ± 7.32 %, and the high encapsulation efficiency greatly increased the amount of Dox that reached the tumor site, thereby improving the tumor therapeutic effect of the LA–PEG–G–Dox nanomedicine.

The Dox can release from LA–PEG–G–Dox nanomedicine which is an important prerequisite to play the antitumor effect after the LA–PEG–G–Dox nanomedicine enters the body. The rapid proliferation of tumor cells in the tumor site consumes a large amount of energy, and the incomplete oxidation of energy produces a large amount of lactic acid, making the environment of the tumor site slightly acidic. The release behavior of Dox from the LA–PEG–G–Dox nanomedicine was studied using different pH values at 37 °C. The Dox release from the LA–PEG–G–Dox nanomedicine was relatively slow, and no sudden release was observed, as shown in **Figure 2**. Simultaneously, the cumulative release amount under the condition of pH 5.0 was larger than that at pH 7.4, which suggested that the Dox released from LA–PEG–G–Dox nanomedicine was more favorable under micro-acid conditions.

This may be due to the fact that Dox easily forms Dox·HCl under low pH conditions, resulting in a greater amount of Dox released from LA–PEG–G–Dox compared with that under high pH condition. The in vitro release experiments demonstrated that Dox can be released well from LA–PEG–G–Dox nanomedicine, which laid the foundation for further experiments. Simultaneously, the release behavior can induce LA–PEG–G–Dox nanomedicine to aggregate in the tumor tissue, decreasing the damage of Dox to normal tissue.

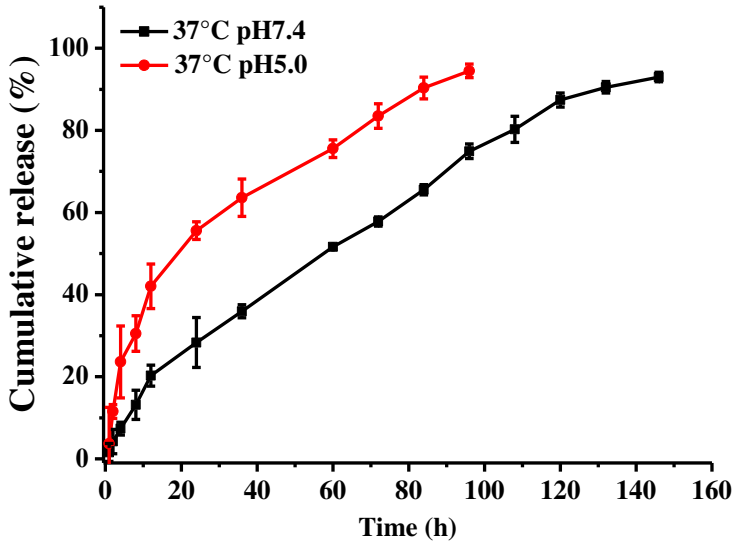

Figure 2 The in vitro release behavior of Dox from the LA–PEG–G–Dox nanomedicine at 37 °C in pH 7.4 and pH 5.0.

3.3 Cytotoxicity of the LA–PEG–G Aggregates and Anticancer Effect of the LA–PEG–G–Dox Nanomedicine in In Vitro

In vitro release experiments showed that Dox can be slowly released from the LA–PEG–G–Dox nanomedicine, and the relative cell viability of LA–PEG–G aggregates and the anticancer activity of LA–PEG–G–Dox nanomedicine were further studied through cell experiments. MCF-7 and HepG2 (human hepatoma cells) were chosen as the model cells for the cell experiment. The cell viability and anticancer activity of nanomedicine were determined with the MTT method, as shown in **Figure 3**. As a drug carrier, LA–PEG–G–Dox's side effects should be considered. The relative cell viability values of both cells were above 90 %, even when the concentration of LA–PEG–G aggregates was 35 μg/mL for 24 h of incubation

(Figures 3a and 3b), which indicated that the cell toxicity of LA–PEG–G aggregates was low. Thus, LA-PEG-G aggregates can be used as drug carriers to encapsulate anticancer drugs to exert antitumor effects. The relative cell viability decreased with increasing LA–PEG–G–Dox nanomedicine concentration after 24 h incubation with MCF-7 **(Figure 3c)** and HepG2 cells **(Figure 3d)**, and the relative cell viability was both about 85 % when the concentration of LA–PEG–G–Dox nanomedicine arrived at 20 μg/mL. Compared with the Dox group, the relative cell viability was about 30 % when the concentration of Dox was 20 μg/mL, indicating that the Dox was slowly releases from the LA-PEG-G-Dox nanomedicine to exert antitumor effects, which prolonged the exertion of Dox's antitumor effects. The LA–PEG–G–Dox nanomedicine simultaneously reduced the side effects of Dox which decrease the damage on cells, thereby also reducing the damage of Dox to normal cells during body circulation.

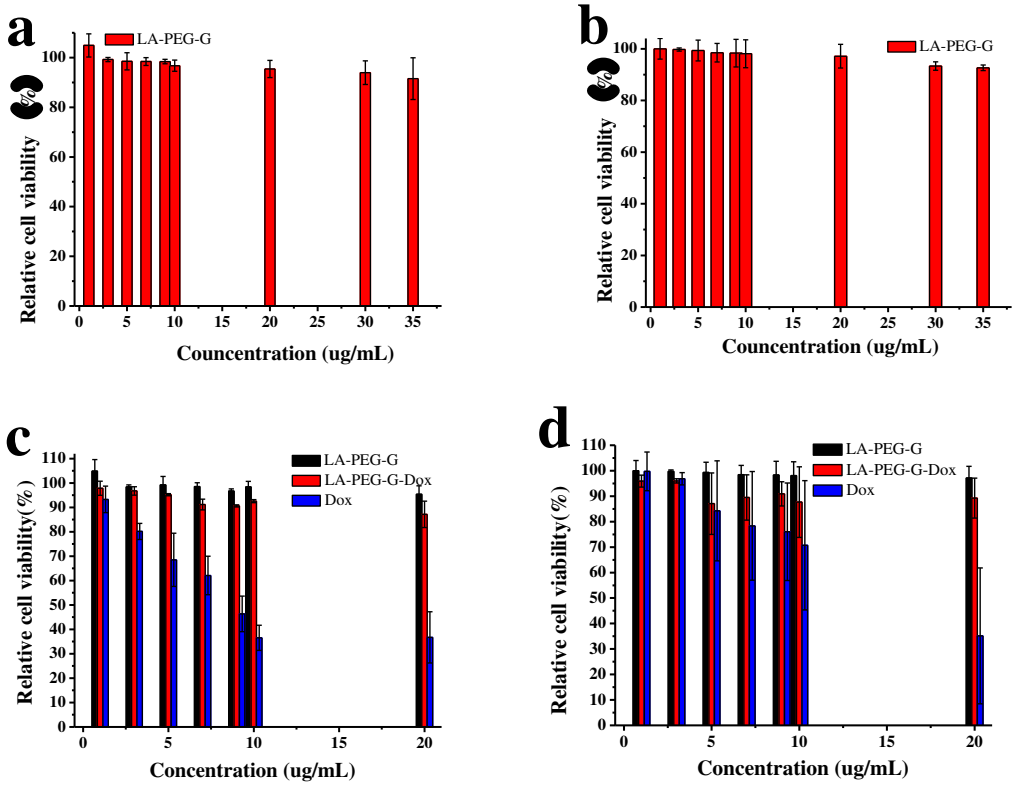

Figure 3. MTT assay. (a) The relative MCF-7 cell viability of LA–PEG–G aggregates for 24 h incubation; (b) The relative HepG2 cell viability of LA–PEG–G aggregates for 24 h incubation; (c) The relative MCF-7 cell viability of LA–PEG–G aggregates, LA–PEG–G–Dox nanomedicine, and Dox group for 24 h incubation; (d) The relative HepG2 cell viability of LA–PEG–G aggregates group, LA–PEG–G–Dox nanomedicine group, and Dox group for 24 h incubation.

3.4 Cell Uptake

HepG2 cells was used to study the cell uptake of LA–PEG–G–Dox nanomedicine with the LSCM and FCM[27]. The Dox can emit the red fluorescence under the 490 nm excitation light. Thus, the Dox uptake behavior can be detected based on the Dox fluorescence signal. LA–PEG–G–Dox nanomedicine at 10 $\mu g \cdot mL^{-1}$ and 20 $\mu g \cdot mL^{-1}$ was incubated with the HepG2 cells for 2 h, 10 h, and 24 h. The LSCM image and FCM assay were shown in the Figure 4. The fluorescence intensity gradually increased with the time increasing as shown in **Figure 4**. The fluorescence initially appeared on the cell surface **(Figure 4a)** at the lower LA–PEG–G–Dox nanomedicine concentration (10 $\mu g \cdot mL^{-1}$) for 2 h incubation, then in the cytoplasm at 8 h **(Figure 4b)**, and even in the nucleus at 24 h **(Figure 4c)**. However, the higher LA–PEG–G–Dox nanomedicine concentration (20 $\mu g \cdot mL^{-1}$) can rapidly enter into the cytoplasm and nucleus, and the fluorescence intensity was also higher than that of 10 $\mu g \cdot mL^{-1}$ LA–PEG–G–Dox nanomedicine group, as shown in **Figures 4d, 4e, and 4f**. Simultaneously, the cell morphology also changed, and the cells became round and condensed. Apoptosis gradually occurred. FCM assay was performed to quantify the cell uptake of the LA–PEG–G–Dox nanomedicine to further verify the cellular uptake. The experimental results are shown in **Figures 4g and Figures S6**. The experimental results showed that the Dox fluorescence signal in the cells increased with time. The fluorescence signal intensity of 20 $\mu g \cdot mL^{-1}$ group was higher than that of the 10 $\mu g \cdot mL^{-1}$ group, and the experimental results were consistent with the above results, as shown in **Figures 4g and S6**. Cell uptake experiments showed that the LA–PEG–G–Dox nanomedicine can gradually enter the cells with the prolong of incubation time of LA–PEG–G–Dox nanomedicine and HepG2 cells, whereas the LA–PEG–G–Dox nanomedicine can effectively induce cancer cell apoptosis. Cell uptake experiments showed that LA–PEG–G–Dox nanomedicine can aggregate at tumor sites and Dox can be slowly release to exert antitumor effects. With the time increasing, the amount of Dox entering tumor cells increased, and further entered the nucleus to induce the cancer cell apoptosis.

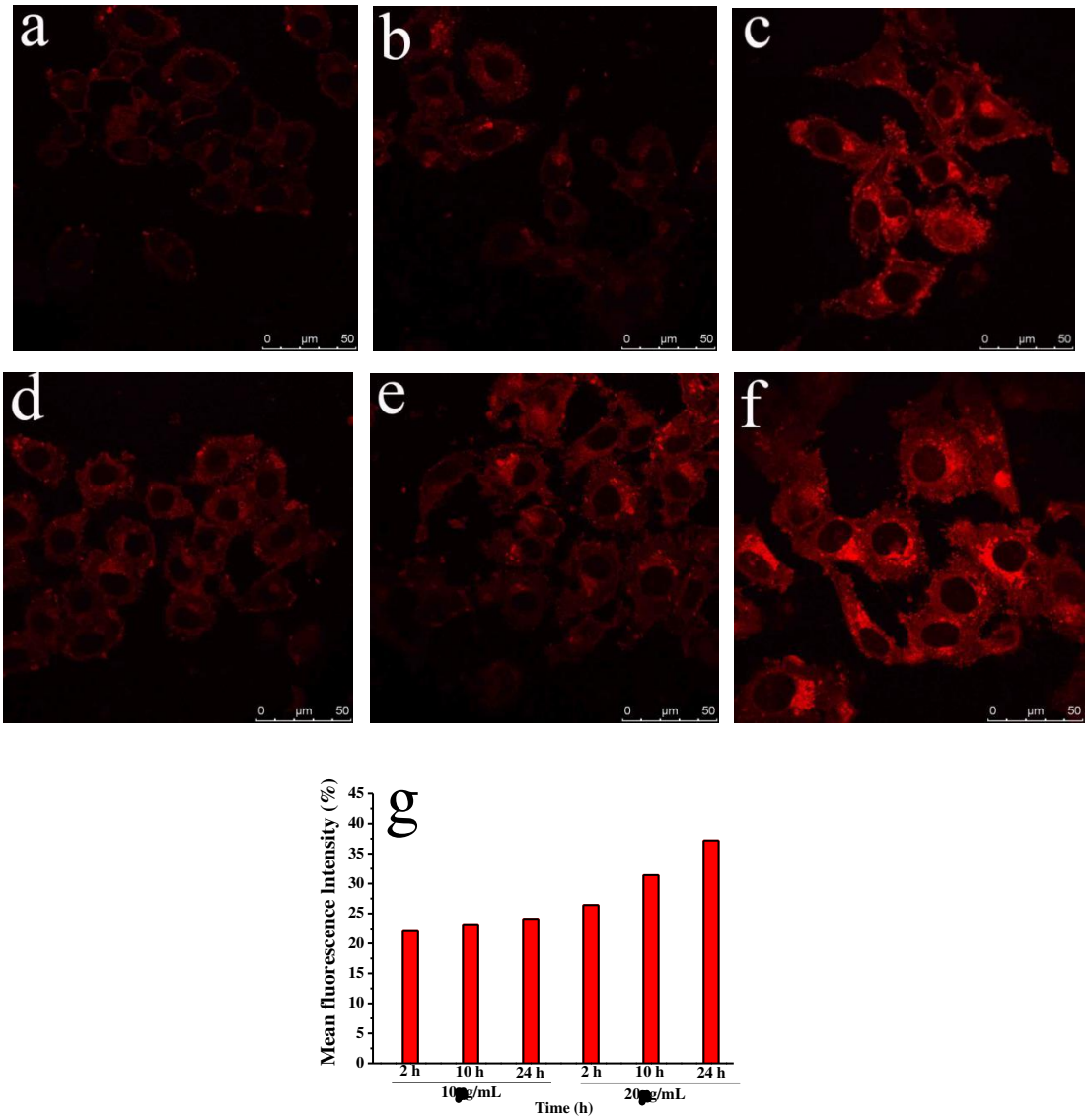

Figure 4. LSCM images and FCM assay. (a) LSCM images of 10 μg·mL^{-1} β-CD-LA-Dox nanomedicine incubated with HepG2 cells for 2 h; (b) LSCM images of 10 μg·mL^{-1} of β-CD-LA-Dox nanomedicine incubated with HepG2 cells for 8 h; (c) LSCM images of 10 μg·mL^{-1} of β-CD-LA-Dox nanomedicine incubated with HepG2 cells for 24 h; (d) 20 μg·mL^{-1} β-CD-LA-Dox nanomedicine incubated with HepG2 cells for 2 h (e) 20 μg·mL^{-1} of β-CD-LA-Dox nanomedicine incubated with HepG2 cells for 8 h; (f) 20 μg·mL^{-1} of β-CD-LA-Dox nanomedicine incubated with HepG2 cells for 24 h; (g) FCM assay of 10 and 20 μg·mL^{-1} LA-PEG-G-Dox nanomedicine incubated with HepG2 cells for 2 h, 8 h and 24 h.

3.5 Antitumor Activity in Vivo and Blood Chemistry

The in vivo antitumor activity of LA–PEG–G aggregates and LA–PEG–G–Dox nanomedicine was further studied with tumor-bearing mice [29]. The tumor-bearing mice were randomly divided into four groups with five mice each group. Every mouse was numbered for subsequent animal experiments. The PBS, LA–PEG–G aggregate solution, and LA–PEG–G–Dox nanomedicine solutions were injected into the

tumor-bearing mice through the tail vein. The body weight and tumor volume of mice were measured to observe the change of body weight and volume of mice after the injection. The tumor volume of PBS **(Figures 5a and 5e)** and LA–PEG–G aggregate group **(Figures 5b and 5f)** became significantly larger than the LA–PEG–G–Dox **(Figures 5c and 5g)** and Dox group **(Figures 5d and 5h)** after 19 days. The tumor of LA–PEG–G–Dox and Dox group had transferred from the forelimb to the entire forelimb, and even to the back of mice. Moreover, some tumors had ruptured. Compared the PBS with LA–PEG–G aggregate group, the tumor volume change of LA–PEG–G–Dox and Dox group was smaller, which indicated that the LA–PEG–G–Dox have evident anticancer effect. In order to observe the size change of the mice tumor, the mice were sacrificed after 19 days, and the tumor of the mice was dissected. The tissue section was shown in **Figure S7**. The changes in tumor volume were clearly observed from the pictures. The tumor volume of the mice in the PBS and LA–PEG–G aggregate group was significantly larger than those in the LA–PEG–G–Dox nanomedicine and Dox group **(Figure S7)**. LA–PEG–G–Dox nanomedicine has the effect of inhibiting tumor increasing, which can effectively inhibit tumor metastasis, and prolong the life span of tumor-bearing mice. As seen from the **Figure 5i**, the mice body weight of PBS and LA–PEG–G aggregate group slightly increased. **The reason may be that the tumor increased**, thereby inducing a gain in the mice body weight and accelerating death. The mice body of Dox group slightly decreased（**Figure 5i**）, and the reason may be that Dox cytotoxicity which affects the mice body. However, the LA–PEG–G–Dox nanomedicine group **(Figure 5i)** had minimal change in body weight. LA–PEG–G–Dox nanomedicine had less toxic side effects on mice and was safer than the other treatment. **Figure 5j** shows the change curve of tumor volume with time. Compared with the LA–PEG–G–Dox nanomedicine and Dox group, the tumor volumes of PBS group and LA–PEG–G aggregate group gradually increased with time. The data were consistent with the change curve of mice body weight. In vivo experiments showed that LA–PEG–G–Dox nanomedicine inhibited tumor growth and metastasis and exerted antitumor effect, and decrease the side effects of Dox.

The tumor and other important organs of mice were studied through the histological section, as shown in **Figures 5k–5n**. Seen from the HE staining results of mouse tumor tissues **(Figures 5k–5n)**, the cells of the tumor tissue sections of the PBS group and LA–PEG–G aggregate group grew vigorously, but tissue necrosis also occurred. The reason may be that the tissue necrosis was caused by insufficient blood supply from tumor growth. Compared with the PBS group **(Figure 5k)**, the range of tumor necrosis increased in the LA–PEG–G aggregate group (Figure 5l), which indicated that the LA–PEG–G aggregate had a certain effect of inhibiting tumor growth [26]. However, LA–PEG–G–Dox nanomedicine **(Figure 5m)** and Dox group **(Figure 5n)** showed that some cells undergo pyknosis, cell nucleus rupture, and cell disintegration, which lead to the extensive necrosis of the tumor tissue. The result indicated that the Dox can release slowly from the LA–PEG–G–Dox nanomedicine to induce the cancer cell apoptosis, and further lead to the large area necrosis of tumor tissue to play the anticancer role. As seen from the tissue sections of heart, liver, spleen, lung, and kidney **(Figure S7)**, the difference of the tissue sections of heart, lung, and spleen were not found between PBS, LA–PEG–G aggregates, LA–PEG–G–Dox nanomedicine and Dox group, which suggested that PBS, LA–PEG–G aggregates, LA–PEG–G–Dox nanomedicine, and Dox were not toxic to the tissue of heart, liver, spleen, lung, and kidney. Compared the PBS and LA–PEG–G aggregate group with the Dox and LA–PEG–G–Dox nanomedicine group, edemas were found in the liver tissue sections of the Dox group and LA–PEG–G–Dox nanomedicine group, which showed that the LA–PEG–G–Dox and Dox was slightly toxic to the liver organ. Hemosiderin was found in the spleen tissue sections in Dox group, but not in the PBS, LA–PEG–G aggregates, and LA–PEG–G–Dox nanomedicine groups. The reason may be that the use of Dox leads to immune anemia and further causes the aging and disintegration of red blood cells. The deposition of hemosiderin appeared, and it indicated that the Dox had serious toxic side effects to the spleen. In summary, the tissue sections showed that the LA–PEG–G–Dox nanomedicine can reduce the toxicity of Dox and induce tumor cell apoptosis, and further lead to tumor necrosis to play the antitumor effect.

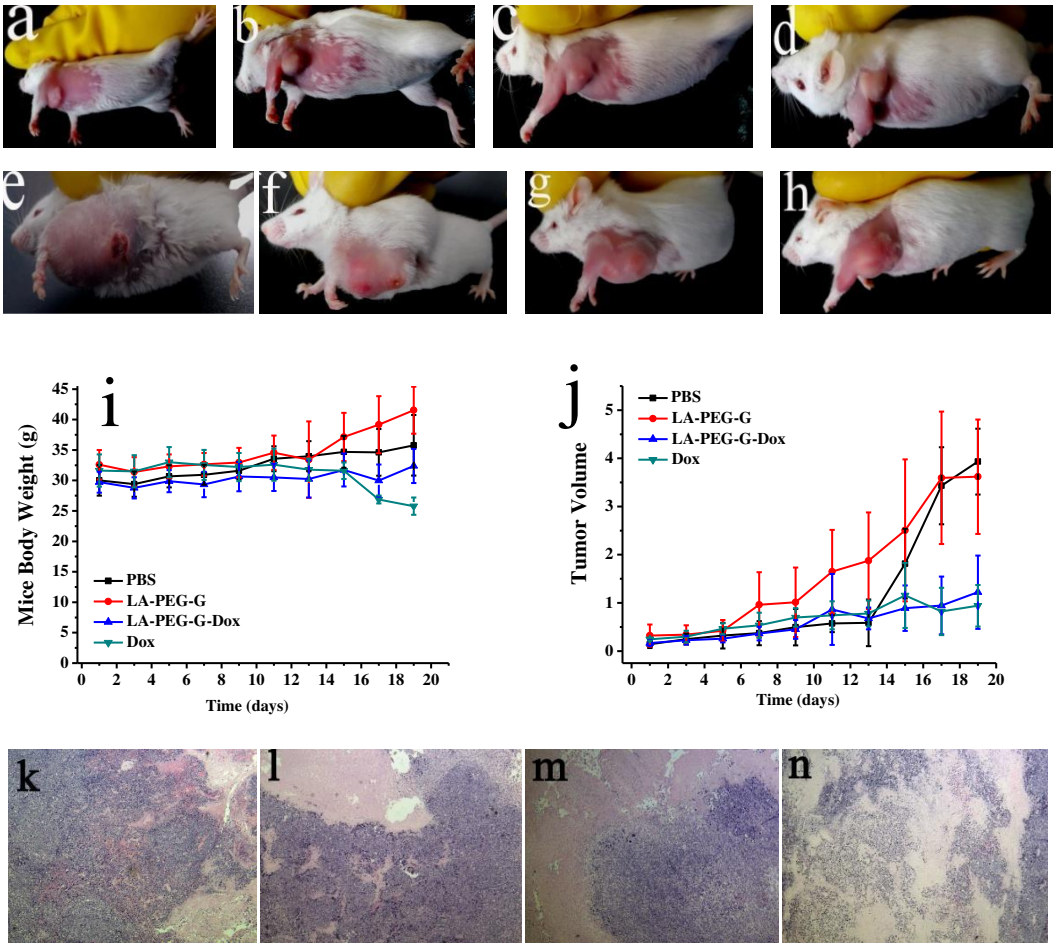

Figure 5. In vivo antitumor efficacy of LA–PEG–G–Dox nanomedicine in mice bearing H22 xenograft tumors. (a) Tumor before injected the PBS; (b) Tumor before injected the LA–PEG–G aggregates; (c) Tumor before injected the LA–PEG–G–Dox nanomedicine; (d) Tumor before injected the Dox; (e) Tumor injected the PBS after 19 days; (f) Tumor injected the LA–PEG–G aggregates after 19 days; (g) Tumor injected the LA–PEG–G–Dox nanomedicine after 19 days; (h) Tumor injected the Dox after 19 days; (i) The mice body weight change with the time increase; (j) The tumor volume change with the time increase; (k)Tissue section of tumor which was injected with PBS after 19 days; (l) Tissue section of tumor was injected with LA–PEG–G aggregates after 19 days; (m) Tissue section of tumor was injected with LA–PEG–G–Dox nanomedicine after 19 days; (n) Tissue section of tumor was injected with Dox after 19 days.

The mice plasmas were collected by the neck-breaking method and then centrifuged to determine the serum biochemistry, and the results were shown in **Table 1.** Seen from the **Table 1**, liver function test showed that alanine aminotransferase (ALT), albumin (ALB), and total bilirubin (TBIL) of the PBS group were lower than other groups, which indicated that the growth of solid tumor did not cause the damage of liver. In contrast, the three indicators of the Dox group were higher than the other groups, and it indicated that the Dox group caused serious damage to the liver of mice due to toxic side effects. Globulin changes in all groups were not obvious, which

indicated that the tumor had no effect on the immune system of mice. The three indicators of LA–PEG–G group (ALT, ALB, and TBIL) were higher than PBS group and lower than the Dox group, and it indicated that the toxicity of LA–PEG–G was low. Moreover, LA–PEG–G–Dox group data showed that the LA–PEG–G–Dox can reduce the Dox toxicity of the liver. The renal function test showed that the solid tumor did not cause renal damage in the PBS group, and the DOX group had the highest urea nitrogen (BUN) and uric acid (UA) content due to the side effects of renal dysfunction. The content of BUN and UA of the LA–PEG–G and LA–PEG–G–Dox groups was lower than that the DOX group, and it suggested that LA–PEG–G–Dox nanomedicine reduced the Dox toxicity to kidney. LA–PEG–G–Dox nanomedicine exerted anticancer effect while protecting the kidneys. The myocardial enzyme test data showed that although the Dox group had an antitumor effect, it had severe cardiotoxicity. In addition, the PBS group had a higher content of AST and α-HBDH due to the growth of solid tumors. The contents of AST and α-HBDH in LA–PEG–G–Dox and LA–PEG–G group were significantly lower than those in PBS and Dox group, and it indicated that LA–PEG–G–Dox nanomedicine reduces the cardiotoxicity of Dox and has an antitumor effect. In summary, the serum biochemical tests showed that LA–PEG–G–Dox nanomedicine can reduce Dox toxic side effects and have good antitumor effect.

Table 1 Blood serum chemistry

Serum Biochemical Detection Project	Serum biochemical indicators	PBS group	Dox group	LA-PEG-G group	LA-PEG-G-DOX group
Liver function tests	ALT(U/L)	410±25.35	143.8±19.01	255.1±25.44	107.9±17.56
	ALB(g/L)	23.2±4.76	16.4±3.22	22.4±4.87	22.2±3.54
	GLD(g/L)	39.5±6.43	40.1±6.54	40.3±6.78	40.6±6.32
	TBIL(μmol/L)	5±0.54	4.2±0.34	4.8±0.42	4.5±0.36
Renal function tests	BUN(mmol/L)	7.66±0.43	8.03±0.35	7.06±0.51	7.45±0.49
	UA(μmol/L)	270.6±35.46	257.5±34.32	180±28.79	232.5±35.76
Myocardialenzyme tests	AST(U/L)	794.4±79.65	2035.3±187.97	565.2±75.41	505.7±67.43
	α-HBDH(U/L)	2159.3±218.54	2166±220.01	1725.8±220.46	1969.6±190.78

ALT: Alanine aminotransferase; ALB: Albumin; GLD: Globulin; TBIL: Total bilirubin; BUN: Urea nitrogen; UA: Uric acid; AST: Aspartate aminotransferase; α-HBDH: α-Hydroxybutyrate Dehydrogenase

4. Conclusion

The amphiphilic molecule LA–PEG–G was synthesized as a drug carrier. This amphiphilic molecule can self-assemble to form aggregates in water with a particle size of 40 nm, which can aggregate at the tumor site to exert an antitumor effect. In vitro release experiments proved that Dox release from that LA–PEG–G–Dox nanomedicine was faster at pH 5.0 compared with pH 7.4, and which suggested that the LA–PEG–G–Dox nanomedicine have good pH-responsive release characteristics. Cell experiments showed that the aggregates formed by LA–PEG–G molecules have extremely low cytotoxicity, and LA–PEG–G–Dox nanomedicine has good anticancer activity. In vivo experiments showed that LA–PEG–G aggregates have a certain inhibitory effect on tumor growth, and LA–PEG–G–Dox nanomedicine has a good therapeutic effect on tumors and almost no effect on the weight of mice. The serum biochemical test results suggested that LA–PEG–G–Dox nanomedicine can reduce the side effects of adriamycin on heart, liver, and kidney. In summary, the LA–PEG–G molecule is an ideal drug carrier, and the LA–PEG–G aggregates have important research significance in antitumor treatment.

5. Competing Interests

The authors declare that they have no competing interests.

6. Funding

This study was financially supported by NSFC (Grant No. 21201020), and the Key R&D Program of Shandong province (Grant No. 2019JZZY011104), and the Shandong Projects of Shandong Province Higher Educational Science and Technology Program (Grant No. J16LC19 and No. J15LC01), and Key Research and Development Plan of Yantai (No.2018XSCC050), and the foundation of Key Laboratory of Colloid and Interface Chemistry (Shandong University), Ministry of Education, China(Grant No. 201703).

7. Acknowledgements

We appreciated Tongshen Liu and Wenbo Liu for the determination of tissue section and TEM image in the manuscript.

8. Consent for Publication

Not applicable.

9. Availability of Data and Material

All data generated or analysed during this study are included in this published article.

10. Authors' Contributions

Guangcheng Wei and Chunhua Wang conceived this system. Guangcheng Wei and Meixiu Xin mainly performed the experiment and and was a major contributor in writing the manuscript. The others assisted to performed the experiment. All authors read and approved the final manuscript.

11. References

[1] C Allemani, T Matsuda and V Di Carlo, et al. Global surveillance of trends in cancer survival 2000-14 (CONCORD-3): analysis of individual records for 37513025 patients diagnosed with one of 18 cancers from 322 population-based registries in 71 countries.*[J]. The. Lancet.*, **2018** ,391, 1023-1075.

[2] Wang Y, Wang L and Yan M, et al. Near-Infrared-Light-Responsive Magnetic DNA Microgels for Photon- and Magneto-Manipulated Cancer Therapy.*[J]. Acs. Appl. Mater. Inter.*, **2017**, 9, 28185-28194.

[3] Liang Y, Deng X and Zhang L, et al. Terminal modification of polymeric micelles with π-conjugated moieties for efficient anticancer drug delivery.*[J]. Biomaterials*, **2015**, 71, 1-10.

[4] Nummelin S, Liljeström V and Saarikoski E, et al. Self-Assembly of Amphiphilic Janus Dendrimers into Mechanically Robust Supramolecular Hydrogels for Sustained Drug Release.*[J]. Chem.Eur.J.*, **2015**, 21, 14433-14439.

[5] Cai A, Wang C and Yan M, et al. A liposome preparation based on β-CD-LPC molecule and its application as drug delivery system.*[J]. Nanomedicine*, **2018**, 13, 2777-2789.

[6] Aslan B, Ozpolat B and Anil K Sood, et al, Gabriel Lopez-Berestein. Nanotechnology in cancer therapy.*[J]. J. Drug Target*, **2013**, 21, 904-913.

[7] K Raemdonck, K Braeckmans, and J Demeestera, et al. Merging the best of both worlds: hybrid lipid enveloped matrix nanocomposites in drug delivery.*[J]. Chem. Soc. Rev.*, **2014**, 43, 444-472.

[8] Liang C, Ye W and Zhu C, et al. Synthesis of Doxorubicin α-Linolenic Acid

Conjugate and Evaluation of Its Antitumor Activity.*[J]. Mol.Pharm.*, **2014**, 11,1378-1390.

[9] Matsuyama W, Mitsuyama H and Watanabe M, et al. Effects of Omega-3 Polyunsaturated Fatty Acids on Inflammatory Markers in COPD.*[J]. Chest.*, **2005**, 128, 3817-3827.

[10] Vladimir P. Torchilin. Lipid-Core Micelles for Targeted Drug Delivery.*[J]. Curr. Drug Deliv*, **2005**, 2,319-327.

[11] Ji Q, Qiu L. Mechanism study of PEGylated polyester and β-cyclodextrin integrated micelles on drug resistance reversal inMRP1-overexpressed HL60/ADR cells.*[J]. Colloid. Surface. B*, **2016**, 144, 203-213.

[12] A P Schmidt, Lara D R and Souza D O. Proposal of a guanine-based purinergic system in the mammalian central nervous system. *[J]. Pharmacol.Therapeut.*, **2007**, 116,401-416.

[13] Frizzo M E S, Lara D. R. and Dahm K C S, et al. Activation of glutamate uptake by guanosine in primary astrocyte cultures.*[J]. Neuroreport*, **2001**, 12, 879-881.

[14] Lanznaster D, Tharine Dal-Cim and Tetsadê C B Piermartiri, et al. Guanosine: a Neuromodulator with Therapeutic Potentialin Brain Disorders.*[J]. Aging. Dis.*, **2016**, 7, 657.

[15]Hansel G, Ramos D B and Delgado C A, et al. The Potential Therapeutic Effect of Guanosine after Cortical Focal Ischemia in Rats.*[J]. Plos.One.,* **2014**,9,e90693-90703.

[16] André Q S, L D Bobermin and D G de Souza, et al. Gliopreventive effects of guanosine against glucosed eprivation in vitro.*[J]. Purinerg.Signal.* , **2013**, 9,643-654.

[17] Lara D R, A P Schmidt and Frizzo M E S, et al. Effect of orally administered guanosine on seizures and death induced by glutamatergic agents.*[J]. Brain.Res.*, **2001**, 912, 176-180.

[18] A P Schmidt, Lara D R. and Maraschin J D F, et al. Guanosine and GMP prevent seizures induced by quinolinic acid in mice.*[J]. Brain. Res.*, **2000**, 864, 40-43.

[19] Ganzella M, Oliveira E D A D and Comassetto D D, et al. Effects of chronic guanosine treatment on hippocampal damage and cognitive impairment of rats

submitted to chronic cerebral hypoperfusion.*[J]. Neurol.Sci.*, **2012**, 33, 985-997.

[20] Lovell J F, Jin C S and Huynh E, et al. Porphysome nanovesicles generated by porphyrin bilayers for use as multimodal biophotonic contrast agents.*[J]. Nat.Mater.*, **2011**, 10,324-332.

[21] Qiu L, Yan L and Zhang L, et al. Folate-modified poly(2-ethyl-2-oxazoline) as hydrophilic corona in polymeric micelles for enhanced intracellular doxorubicin delivery.*[J]. Int.J.Pharm.*, **2013**, 456, 315-324.

[22] Tan H W and Misran M. Polysaccharide-anchored fatty acid liposome.*[J]. Int.J.Pharm.*, **2013**, 441,414-423.

[23] Tannock I F and Rotin D. Acid pH in Tumors and Its Potential for Therapeutic Exploitation.*[J]. Cancer.Res.*, **1989**, 49,4373-4384.

[24] Yan M, Cai A and Li J, et al. Preparation of β-CD-DPPE-Dox Nanomedicine and Its' Application as the Anticancer and Antitumor Drug.*[J]. Sci. Rep-UK.*, **2019**, 9(1). doi:10.1038/s41598-019-50162-8.

[25] Li J, Xin M and Huo Y, et al. Synthesis of β-cyclodextrin-PEG-G Molecules to Delay Tumor Growth and Application of β-cyclodextrin-PEG-G Aggregates as Drug Carrier. *[J]. Carbohyd. Polym.* , **2019**, 115478. doi:10.1016/j.carbpol.2019.115478 .

[26] Sun B, Luo C and Cui W, et al. Chemotherapy agent-unsaturated fatty acid prodrugs and prodrug nanoplatforms for cancer chemotherapy.*[J]. J.Control Release*, **2017**, 264,145-159.

[27] Wang W, Shao A and Zhang N, et al. Cationic Polymethacrylate Modifed Liposomes Signifcantly Enhanced Doxorubicin Delivery and Antitumor Activity.*[J]. Sci. Rep-UK.*, **2017**, 7, 43036-43046.

[28] Xu P, Zuo H and Chen B, et al. Doxorubicin-loaded platelets as a smart drug delivery system: An improved therapy for lymphoma.*[J]. Sci. Rep-UK.*, **2017**, 7, 42632-42647.

Supplementary Files

This is a list of supplementary files associated with this preprint. Click to download.

- SupportingInformation201918.docx